



Research Article

ISSN : 0975-7384  
CODEN(USA) : JCPRC5

## Electrochemical impedance spectroscopy weight loss and quantum chemical study of new pyridazine derivative as inhibitor corrosion of copper in nitric acid

A. Zarrouk<sup>1</sup>, H. Zarrok<sup>2</sup>, R. Salghi<sup>3</sup>, R. Touri<sup>4</sup>, B. Hammouti<sup>1</sup>, N. Benchat<sup>1</sup>, L. L. Afrine<sup>5</sup>,  
H. Hannache<sup>5</sup>, M. El Hezzat<sup>6</sup> and M. Bouachrine<sup>7</sup>

<sup>1</sup>LCAE-URAC 18, Faculty of Science, University of Mohammed Premier, Oujda, Morocco

<sup>2</sup>Laboratory Separation Processes, Faculty of Science, University Ibn Tofail, Kenitra, Morocco

<sup>3</sup>Laboratory of Environmental Engineering and Biotechnology, ENSA, University Ibn Zohr, Agadir, Morocco

<sup>4</sup>Materials, Electrochemical and Environment Laboratory, Faculty of Science, University Ibn Tofail, Kenitra, Morocco

<sup>5</sup>Laboratoire d'Ingénierie et Matériaux: Equipe des Matériaux Thermo-Structuraux et Polymères, Université Hassan II-Mohammedia, Faculté des Sciences Ben M'Sik, Casablanca, Maroc

<sup>6</sup>Laboratoire de Physico-Chimie du Solide (LPCS), Faculté des Sciences, Université Ibn Tofail, Kenitra, Morocco

<sup>7</sup>ESTM, Université Mouly Ismail, Meknes, Morocco

---

### ABSTRACT

The performance of 5-[(2-chlorophenyl)(hydroxy)methyl]-6-methylpyridazin-3(2H)-one (P4) as corrosion inhibitor for copper corrosion in 2.0 M HNO<sub>3</sub> solutions in the temperature range from 303K to 343K was investigated weight loss, electrochemical impedance spectroscopy (EIS) technique and quantum chemical study. The results obtained from the both measurement techniques revealed good inhibitor efficiency in the studied concentration range. The inhibition efficiency decrease with rise in temperature. Impedance measurements showed that the double-layer capacitance decreased and charge-transfer resistance increased with increase in the inhibitor concentration and hence increasing in inhibition efficiency. The free energy of adsorption and the influence of temperature on the adsorption of inhibitor onto copper surface have been reported. The adsorption of the P4 was found to obey the Langmuir adsorption isotherm. Further, theoretical calculations were carried out and relations between computed parameters and experimental inhibition efficiency were discussed.

**Keywords:** Inhibitor, Copper, HNO<sub>3</sub>, EIS, Gravimetric

---

### INTRODUCTION

Organic inhibitors were applied extensively to protect metals from corrosion in many aggressive acidic media (e.g. in the acid pickling and cleaning processes of metals) [1-3]. Organic compounds containing N, S and O atoms [4-31] were found to be good corrosion inhibitors of metals particularly for active metals like Fe, Cu etc. The effectiveness of these compounds as corrosion inhibitors has been interpreted in terms of their molecular structure, molecular size, and molecular mass, hetero-atoms present and adsorptive tendencies [32]. Under certain conditions, the electronic structure of the organic inhibitors has a key influence on the corrosion inhibition efficiency to the metal. The inhibitors influence the kinetics of the electrochemical reactions which constitute the corrosion process and thereby modify the metal dissolution in acids. The existing data show that most organic inhibitors act by adsorption on the metal surface. They change the structure of the electrical double layer by adsorption on the metal surface. Quite a number of studies have been carried out in determination of adsorptivity of various compounds at the electrode/solution interface [33-34].

This article reported our attempt to use electrochemical impedance spectroscopy (EIS) and theoretical calculations to investigate the corrosion inhibition effect of 5-[(2-chlorophenyl)(hydroxy)methyl]-6-methylpyridazin-3(2H)-one (P4) on the copper surface. The structure of pyridazine derivative is shown in Figure 1.

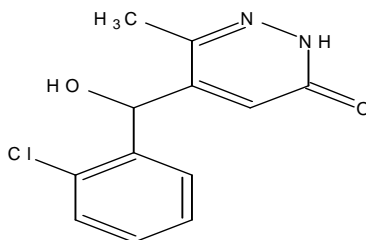


Figure 1. The chemical structure of the studied pyridazine derivative compound

## EXPERIMENTAL SECTION

### Materials and reagents

Copper strips containing 99.5 wt.% Cu, 0.001wt.% Ni, 0.019 wt.% Al, 0.004 wt.% Mn, 0.116 wt.% Si and balance impurities were used for electrochemical and gravimetric studies. The Copper samples were mechanically polished using different grades of emery paper, washed with double distilled water, and dried at room temperature. Appropriate concentration of aggressive solutions used (2.0 M HNO<sub>3</sub>) was prepared using double distilled water.

### Weight loss measurements

The copper sheets of 2 cm × 2 cm × 0.20 cm dimensions were abraded with different grades of emery papers, washed with distilled water, degreased with acetone, dried and kept in a desiccator. After weighing accurately by a digital balance with high sensitivity the specimens were immersed in solution containing 2.0 M HNO<sub>3</sub> solution with and without various concentrations of the investigated inhibitor. At the end of the tests, the specimens were taken out, washed carefully in ethanol under ultrasound until the corrosion products on the surface of copper specimens were removed thoroughly, and then dried, weighed accurately. Duplicate experiments were performed in each case and the mean value of the weight loss is reported. Weight loss allowed calculation of the mean corrosion rate in mg cm<sup>-2</sup> h<sup>-1</sup>. The corrosion rate ( $v$ ), surface coverage ( $\theta$ ) and the inhibition efficiency ( $\eta_{WL}$ ) were calculated by the following equations:

$$v = \frac{W}{St} \times 100 \quad (1)$$

$$\theta = \frac{v_0 - v}{v_0} \quad (2)$$

$$\eta_{WL} (\%) = \frac{v_0 - v}{v_0} \times 100 \quad (3)$$

where  $W$  is the three-experiment average weight loss of the copper,  $S$  is the total surface area of the specimen,  $t$  is the immersion time and  $v_0$  and  $v$  are values of the corrosion rate without and with addition of the inhibitor, respectively.

### Electrochemical impedance spectroscopy

The electrochemical measurements were carried out using Volta lab (Tacussel- Radiometer PGZ 301) potentiostat and controlled by Tacussel corrosion analysis software model (Voltmaster 4) at under static condition. The corrosion cell used had three electrodes. The reference electrode was a saturated calomel electrode (SCE). A platinum electrode was used as auxiliary electrode of surface area of 1 cm<sup>2</sup>. The working electrode was copper. All potentials given in this study were referred to this reference electrode. The working electrode was immersed in test solution for 30 minutes to establish steady state open circuit potential ( $E_{ocp}$ ). After measuring the  $E_{ocp}$ , the electrochemical measurements were performed. All electrochemical tests have been performed in aerated solutions at 303 K. The EIS experiments were conducted in the frequency range with high limit of 100 kHz and different low limit 0.1 Hz at open circuit potential, with 10 points per decade, at the rest potential, after 30 min of acid immersion, by applying 10 mV ac voltage peak-to-peak. Nyquist plots were made from these experiments. The best

semicircle can be fit through the data points in the Nyquist plot using a non-linear least square fit so as to give the intersections with the  $x$ -axis.

### Quantum chemical calculations

Complete geometrical optimizations of the investigated molecules are performed using DFT (density functional theory) with the Beck's three parameter exchange functional along with the Lee-Yang-Parr nonlocal correlation functional (B3LYP) [35-37] with 6-31G\* basis set is implemented in Gaussian 03 program package [38]. This approach is shown to yield favorable geometries for a wide variety of systems. This basis set gives good geometry optimizations. The geometry structure was optimized under no constraint. The following quantum chemical parameters were calculated from the obtained optimized structure: the energy of the highest occupied molecular orbital ( $E_{\text{HOMO}}$ ), the energy of the lowest unoccupied molecular orbital ( $E_{\text{LUMO}}$ ),  $\Delta E_{\text{gap}} = E_{\text{HOMO}} - E_{\text{LUMO}}$ , the dipole moment ( $\mu$ ) and total energy (TE).

## RESULTS AND DISCUSSION

### Weight loss

#### Effect of temperature

The effect of temperature on the inhibition efficiency of the P4 for copper in 2.0 M  $\text{HNO}_3$  solution in the absence and presence of optimum concentration ( $10^{-3} \text{ mol L}^{-1}$ ) at temperature ranging from 303 to 343 K was investigated by weight loss measurements. The results obtained are given in Table 1 and plot between inhibition efficiency vs temperature is shown in Fig. 2.

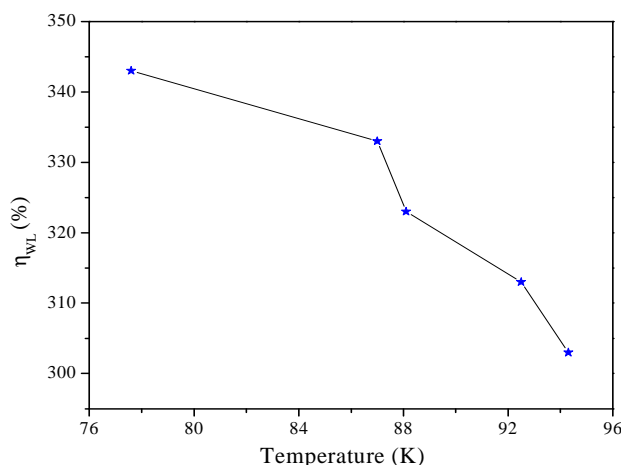


Figure 2. Variation of inhibition efficiency with Temperature

Table 1. Various corrosion parameters for copper in 2.0 M  $\text{HNO}_3$  in absence and presence of optimum concentration of P4 at different temperatures at 1h

Temperature (K)	Inhibitor	$v$ ( $\text{mg}/\text{cm}^2 \text{ h}$ )	$\eta_{\text{WL}}$ (%)	$\theta$
303	Blank	1.78	-----	-----
	P4	0.10	94.3	0.943
313	Blank	7.33	-----	-----
	P4	0.55	92.5	0.925
323	Blank	24.97	-----	-----
	P4	2.97	88.1	0.881
333	Blank	70.82	-----	-----
	P4	9.24	87.0	0.870
343	Blank	186.61	-----	-----
	P4	41.85	77.6	0.776

It is observed that as the temperature increases from 303 to 343 K inhibition efficiency decreases while corrosion rate increases. This behavior can be explained on the basis that the increase in temperature causes the desorption of the inhibitor molecules from the surface of copper.

**Thermodynamic activation parameters and adsorption isotherm**

In order to find the activation parameters of the corrosion inhibition process for copper in 2.0 M HNO<sub>3</sub> solution, weight loss measurements were performed at a temperature range 303 to 343 K in the absence and presence of 10<sup>-3</sup> mol L<sup>-1</sup> pyridazine derivative. A plot of the logarithm of the corrosion rate (mg cm<sup>-2</sup> h<sup>-1</sup>) of copper vs. 1000/T gave a straight line as shown in Fig.3

According to the Arrhenius equation:

$$v = A \exp\left(\frac{-E_a}{RT}\right) \quad (4)$$

where  $E_a$  is the apparent activation energy for the corrosion of copper in 2.0 M HNO<sub>3</sub> solution,  $R$  molar gas constant,  $A$  the Arrhenius pre-exponential factor and  $T$  is the absolute temperature. The values of  $E_a$  obtained from the slope of the line (Fig. 3) are given in Table 2.

From table 2 it is clear that activation energy of P4 is higher (128.70 kJ mol<sup>-1</sup>) as compare to blank acid solution (100.21 kJ mol<sup>-1</sup>) this show that corrosion rate of copper is mainly controlled by activation energy [39].

The straight lines were obtained according to the transition state equation:

$$v = \frac{RT}{Nh} \exp\left(\frac{\Delta S_a}{R}\right) \exp\left(-\frac{\Delta H_a}{RT}\right) \quad (5)$$

Where  $N$  is the Avogadro's number,  $h$  the Plank's constant,  $\Delta H_a$  the enthalpy of activation and  $\Delta S_a$  the entropy of activation.

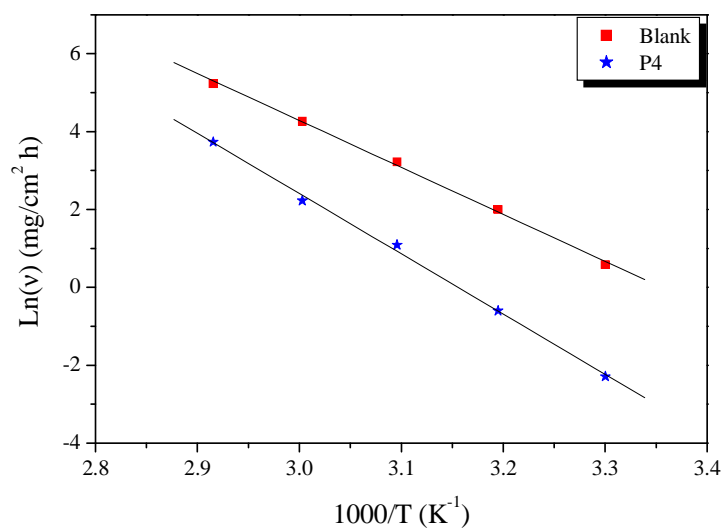


Figure 3. Arrhenius plot of copper in 2.0 HNO<sub>3</sub> in absence and presence of different concentration of P4

Table 2. Thermodynamic parameters for copper in 2.0 HNO<sub>3</sub> in absence and presence of optimum concentration (10<sup>-3</sup> M) of P4 (inhibitor)

Tem (K)	Free acid			P4 (10 <sup>-3</sup> M)			K <sub>ads</sub> (M <sup>-1</sup> )	ΔG <sub>ads</sub> (kJ/mol)
	E <sub>a</sub> (KJ/mol)	ΔH <sub>a</sub> (kJ/mol)	ΔS <sub>a</sub> (J/mol K)	E <sub>a</sub> (KJ/mol)	ΔH <sub>a</sub> (kJ/mol)	ΔS <sub>a</sub> (J/mol K)		
303							16543.9	-34.59
313							12306.7	-34.96
323	100.21	097.53	082.36	128.70	126.02	152.24	7403.4	-34.71
333							6692.3	-35.51
343							3464.3	-34.96

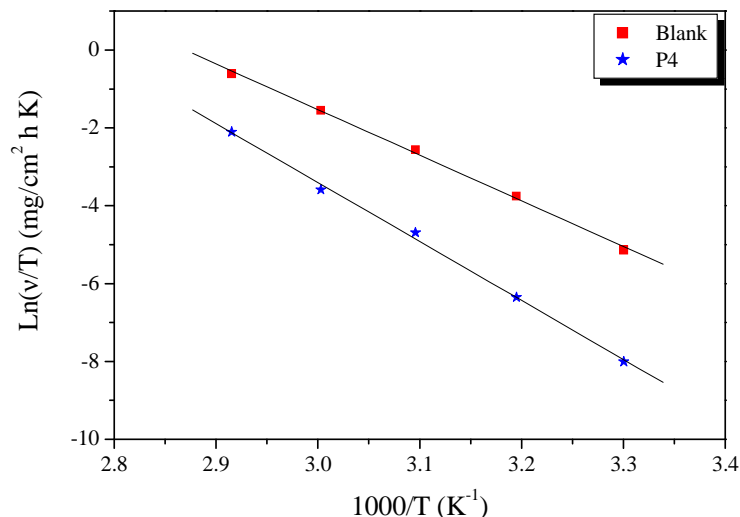


Figure 4. Transition-state plot of copper in 2.0 HNO<sub>3</sub> in absence and presence of optimum concentration of P4

Fig 5. shows that a plot of  $\ln(v/T)$  versus  $1000/T$  gives a straight line with a slope of  $(-\Delta H_a/R)$  and an intercept of  $\ln(R/Nh + \Delta S_a/R)$  from which the values of  $\Delta H_a$  and  $\Delta S_a$  are calculated and are given in Table 2.

Table 2 shows that value of enthalpy of activation is positive and higher in presence of inhibitor. The positive sign of  $\Delta H_a$  reflects the endothermic nature of the copper dissolution process suggesting that the dissolution of copper is slow. The entropy of activation  $\Delta S_a$  is higher ( $152.24 \text{ J K}^{-1} \text{ mol}^{-1}$ ) in the presence of inhibitor than that ( $82.36 \text{ J K}^{-1} \text{ mol}^{-1}$ ) in the absence of the inhibitor. This is opposite to what would be expected, since adsorption of inhibitor is an exothermic process and is always accompanied by a decrease of entropy. The reason could be explained as follows: the adsorption of organic inhibitor molecules from the aqueous solution can be regarded as a quasi-substitution process between the organic compound in the aqueous phase [ $\text{Org}_{(\text{sol})}$ ] and water molecules at the electrode surface [ $\text{H}_2\text{O}_{(\text{ads})}$ ]. In this situation, the adsorption of organic inhibitor is accompanied by desorption of water molecules from the surface. Thus, while the adsorption process for the inhibitor is believed to be exothermic and associated with a decrease in entropy of the solute, the opposite is true for the solvent. The thermodynamic values obtained are the algebraic sum of the adsorption of organic molecules and desorption of water molecules. Therefore, the gain in entropy is attributed to the increase in solvent entropy [40]. The positive values of  $\Delta S_a$  means that the adsorption process is accompanied by an increase in entropy, which is the driving force for the adsorption of inhibitor onto the copper surface [41].

The standard free energy of adsorption ( $\Delta G_{\text{ads}}^\circ$ ) at different temperatures is calculated from the equation:

$$\Delta G_{\text{ads}}^\circ = -RT \ln(55.55 K_{\text{ads}}) \quad (6)$$

where the value 55.55 is the concentration of water in solution expressed in  $\text{mol L}^{-1}$  [42,43] and  $K_{\text{ads}}$  is equilibrium adsorption constant and is given by:

$$K_{\text{ads}} = \frac{\theta}{C(1-\theta)} \quad (7)$$

where  $\theta$  is degree of surface coverage of the copper surface and  $C$  the molar concentration of inhibitor.

The values of  $K_{\text{ads}}$  and  $\Delta G_{\text{ads}}^\circ$  for in 2.0 HNO<sub>3</sub> solution in the presence of  $10^{-3}$  M P4 is given in Table 2.

The negative values of  $\Delta G_{\text{ads}}^\circ$  ensure the spontaneity of the adsorption process and stability of the adsorbed layer on the copper surface. Generally, values of  $\Delta G_{\text{ads}}^\circ$  around  $-20 \text{ kJ mol}^{-1}$  or lower are consistent with the electrostatic interaction between the charged molecules and charge metal, such as physisorption. When it is around  $-40 \text{ kJ mol}^{-1}$  or higher values it involve charge sharing or charge transfer from organic molecules to the metal surface to form a

coordinate type of bond that is chemisorption [44]. The calculated values range from -35.59 to -35.51 kJ mol<sup>-1</sup> (Table 2). This indicates that P4 are adsorbed physically on copper surface in 2.0 HNO<sub>3</sub> solution.

Attempts were made to fit  $\theta$  values to the Freundlich, Temkin, Langmuir, and Flory-Huggins isotherms, and the correlation coefficient ( $R^2$ ) values were used to determine the best fit isotherm. The best results were obtained for the Langmuir adsorption isotherm. A straight line was obtained on plotting  $C/\theta$  vs.  $C$  (mol L<sup>-1</sup>) as shown in Fig 5.

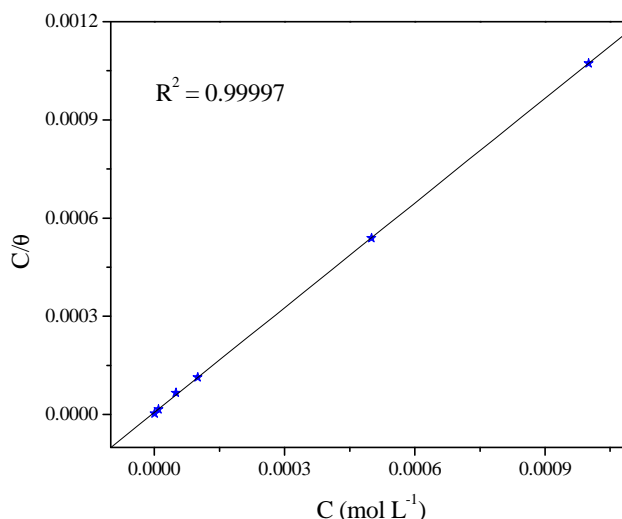


Figure 5. Langmuir's isotherm for adsorption of P4 on copper surface in 2.0 HNO<sub>3</sub>

It suggested that the adsorption of the inhibitor at the metal/solution interface follows Langmuir's adsorption isotherm.

#### **Electrochemical Impedance Spectroscopy**

Impedance spectra for copper in 2.0 HNO<sub>3</sub> solution in absence and presence of different concentrations of P4 at 303 K are shown in the form of Nyquist plots (Fig. 6). In all cases, the Nyquist plots are not perfect semicircles. Deviations of this kind are often referred to as the frequency dispersion of interfacial impedance. This anomalous phenomenon can be attributed to the inhomogeneity of the electrode surface arising from surface roughness or interfacial phenomena [45]. The polarization resistance values  $R_p$  were calculated from the difference in impedance at the lower and higher frequencies, as suggested by Haruyama and Tsuru [46].  $C_{dl}$  values were calculated from the frequency at which the imaginary component of impedance was maximum ( $Z_{im\ max}$ ) using the reaction:

$$C_{dl} = \frac{1}{2\pi f_{max} R_{ct}} \quad (1)$$

Where  $f_{max}$  is the frequency at which the imaginary component of impedance is maximum. The inhibition efficiency of the inhibitor was calculated from the polarization resistance values using the following equation:

$$\% IE = \frac{R_{p(inh)} - R_p}{R_{p(inh)}} \times 100 \quad (2)$$

Where  $R_{p(inh)}$  and  $R_p$  represent the polarization resistance in the presence and absence of inhibitor, respectively.

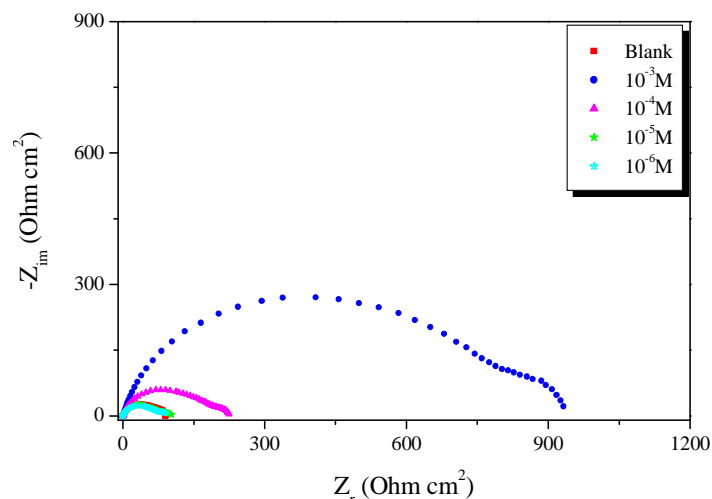


Figure 6. Nyquist diagram of copper in 2.0 M HNO<sub>3</sub> solution in the absence and presence different concentrations of P4 at 303 K

The values of  $R_p$ ,  $C_{dl}$  and %IE for copper in 2.0 M nitri acid containing different concentrations for the used inhibitor are shown in Table 3. The data indicate that increasing polarization resistance is associated with a decrease in the double layer capacitance and increase in the percentage inhibition efficiency. The decrease in  $C_{dl}$  values could be attributed to the adsorption of the inhibitor molecules at the metal surface. It has been reported that the adsorption of organic inhibitor on the metal surface is characterized by a decrease in  $C_{dl}$ . Furthermore the decreased values of  $C_{dl}$  may be due to the replacement of water molecules at the electrode interface by organic inhibitor of lower dielectric constant through adsorption.

Table 3. Corrosion parameters obtained by impedance measurements for copper in 2.0 M HNO<sub>3</sub> at various concentrations of P4

	Conc (M)	$R_p$ ( $\Omega \cdot \text{cm}^2$ )	$f_{\max}$ (Hz)	$C_{dl}$ ( $\mu\text{F}/\text{cm}^2$ )	IE (%)
Blank	2.0	091.4	15.82	110.1	-
P4	$10^{-3}$	930.7	02.81	062.7	90.2
	$10^{-4}$	224.5	10.00	086.1	59.3
	$10^{-5}$	103.8	12.50	151.6	12.0
	$10^{-6}$	097.8	14.04	141.1	06.5

### Quantum Chemical Calculations

The structure and electronic parameters were obtained by means of theoretical calculations using the computational methodologies of quantum chemistry. The optimized molecular structures and frontier molecular orbital density distribution of the studied molecule are shown in Figures 7-8. The calculated quantum chemical parameters such as  $E_{\text{HOMO}}$ ,  $E_{\text{LUMO}}$ ,  $\Delta E_{\text{LUMO-HOMO}}$ , dipole moments ( $\mu$ ) are listed in Table 4. All quantum chemical properties were obtained after geometric optimization with respect to the all nuclear coordinates using Kohn-Sham approach at DFT level. The molecular structure of pyridazine shows that the molecules seems to adsorb on copper surface by sharing of electrons of the nitrogen atoms with copper to form coordinated bonds and  $\pi$ -electron interactions of the aromatic rings.

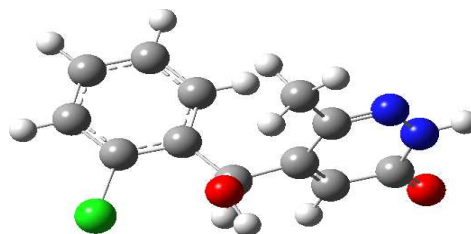


Figure 7. Optimized structure of studied molecule obtained by B3LYP/6-31G\* level

In Fig. 8, we have presented the frontier molecule orbital density distributions of the studied compound. Analysis of Fig. 8 shows that the distribution of two energies HOMO and LUMO, we can see that the electron density of the HOMO and LUMO location was distributed almost of pyridazine ring.

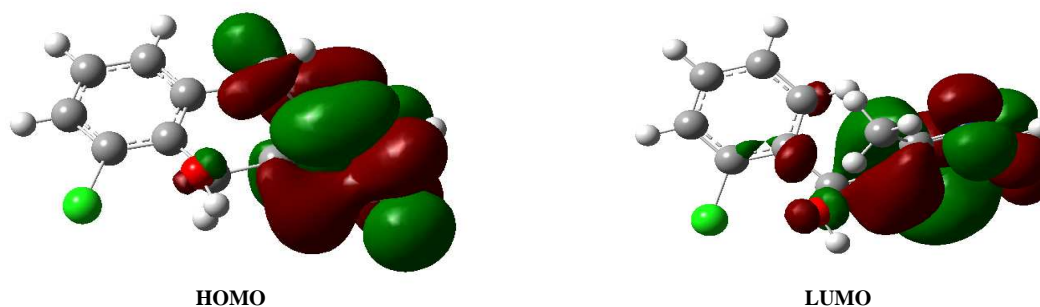


Figure 8. Schematic representation of HOMO and LUMO molecular orbital of studied molecules

Table 4. Calculated quantum chemical parameters of the studied compound.

Quantum parameters	P4
$E_{HOMO}$ (eV)	-6.371
$E_{LUMO}$ (eV)	-1.767
$\Delta E_{gap}$ (eV)	4.604
$\mu$ (debye)	2.1127
TE (eV)	-1177.935

The total energy for our studied molecule calculated by DFT quantum chemical methods is equal to -1177.935 eV. Hohenberg and Kohn [47] proved that the total energy of a system including that of the many body effects of electrons (exchange and correlation) in the presence of static external potential (for example, the atomic nuclei) is a unique functional of the charge density. The minimum value of the total energy functional is the ground state energy of the system. The electronic charge density which yields this minimum is then the exact single particle ground state energy. On the other hand, the transition of electron, according to the frontier molecular orbital theory of chemical reactivity, is due to interaction between highest occupied molecular orbital (HOMO) and lowest unoccupied molecular orbital (LUMO) of reacting species.  $E_{HOMO}$  is a quantum chemical parameter which is often associated with the electron donating ability of the molecule. High value of  $E_{HOMO}$  is likely to a tendency of the molecule to donate electrons to appropriate acceptor molecule of low empty molecular orbital energy [48]. The inhibitor does not only donate electron to the unoccupied d orbital of the metal ion but can also accept electron from the d-orbital of the metal leading to the formation of a feed back bond. The highest value of  $E_{HOMO} = -6.371$  eV of the studied compound indicates the better inhibition efficiency. On the other hand, It has also been found that an inhibitor does not only donate an electron to the unoccupied d orbital of the metal ion but can also accept electrons from the d orbital of the metal leading to the formation of a feedback bond. Therefore, the tendency for the formation of a feedback bond would depend on the value of  $E_{LUMO}$ . The obtained value of the  $E_{LUMO} = -1.767$  eV indicates the easier of the acceptance of electrons from the d orbital of the metal [49,50]. The band gap energy,  $\Delta E = E_{LUMO} - E_{HOMO}$  is an important parameter as a function of reactivity of the inhibitor molecule towards the adsorption on metallic surface. As  $\Delta E$  decreases, the reactivity of the molecule increases leading to increase the inhibition efficiency of the molecule. The calculations indicate that our studied molecule has a small value of gap energy (4.604 eV) which means the highest reactivity and accordingly the highest inhibition efficiency which agrees well with the experimental observations. The dipole moment ( $\mu$  in Debye) is another important electronic parameter that results from non uniform distribution of charges on the various atoms in the molecule. The high value of dipole moment probably increases the adsorption between chemical compound and metal surface [51, 52]. In our study, the value of the dipole moment is 2.1127 debye.

### CONCLUSION

In this study, it was shown that pyridazine derivative (P4), is effective inhibitor of corrosion of copper exposed to 2.0 M  $HNO_3$ . In determining the corrosion rate, electrochemical impedance spectroscopy and weight loss measurements give comparable results. The analysis of degree of surface coverage of this compound showed the linearity of Langmuir isotherm adsorptions, which represent the monolayer formation of this compound on copper surface. The free Gibbs adsorption energy values,  $\Delta G_{ads}^\circ$ , of synthesized compound is negative, which indicated the spontaneity of adsorption process of this compound on copper surface. The correlation between the quantum chemical parameters and inhibition efficiency was investigated using DFT/B3LYP calculations. The inhibition efficiency of the inhibitor are closely related to the quantum chemical parameters, the highest occupied molecular orbital ( $E_{HOMO}$ ), energy of lowest unoccupied molecular orbital ( $E_{LUMO}$ ), HOMO-LUMO energy gap ( $\Delta E_{H-L}$ ), the dipole moment ( $\mu$ ) and the total energy (TE).



## REFERENCES

- [1] G. E. Badr, *Corros. Sci.*, **2009**, 51, 2529.
- [2] Y. Ren, Y. Luo, K. Zhang, G. Zhu, X. Tan, *Corros. Sci.*, **2008**, 50, 3147.
- [3] K. S. Jacob, G. Parameswaran, *Corros. Sci.*, **2010**, 52, 224.
- [4] A. K. Singh, M. A. Quraishi, *J. Mater. Environ. Sci.*, **2010**, 1, 101.
- [5] M. Prajila, J. Sam, J. Bincy, J. Abraham, *J. Mater. Environ. Sci.*, **2012**, 3, 1045.
- [6] U. J. Naik, V. A. Panchal, A. S. Patel, N. K. Shah, *J. Mater. Environ. Sci.*, **2012**, 3, 935.
- [7] A. Zarrouk, H. Zarrok, R. Salghi, B. Hammouti, F. Bentiss, R. Tourir, M. Bouachrine, *J. Mater. Environ. Sci.*, **2013**, 4, 177.
- [8] D. Ben Hmamou, R. Salghi, A. Zarrouk, H. Zarrok, S. S. Al-Deyab, O. Benali, B. Hammouti, *Int. J. Electrochem. Sci.*, **2012**, 7, 8988.
- [9] B. Hammouti, A. Zarrouk, S. S. Al-Deyab and I. Warad, *Orient. J. Chem.*, **27** (2011) 23.
- [10] A. Zarrouk, M. Messali, H. Zarrok, R. Salghi, A. A. Ali, B. Hammouti, S. S. Al-Deyab, F. Bentiss, *Int. J. Electrochem. Sci.*, **2012**, 7, 6998.
- [11] H. Zarrok, A. Zarrouk, R. Salghi, Y. Ramli, B. Hammouti, S. S. Al-Deyab, E. M. Essassi, H. Oudda, *Int. J. Electrochem. Sci.*, **2012**, 7, 8958.
- [12] A. Zarrouk, B. Hammouti, S. S. Al-Deyab, R. Salghi, H. Zarrok, C. Jama, F. Bentiss, *Int. J. Electrochem. Sci.*, **2012**, 7, 5997.
- [13] D. Ben Hmamou, M. R. Aouad, R. Salghi, A. Zarrouk, M. Assouag, O. Benali, M. Messali, H. Zarrok, B. Hammouti, *J. Chem. Pharm. Res.*, **2012**, 4, 3489.
- [14] A. Zarrouk, H. Zarrok, R. Salghi, B. Hammouti, S. S. Al-Deyab, R. Touzani, M. Bouachrine, I. Warad, T. B. Hadda, *Int. J. Electrochem. Sci.*, **2012**, 7, 6353.
- [15] H. Zarrok, R. Saddik, H. Oudda, B. Hammouti, A. El Midaoui, A. Zarrouk, N. Benchat, M. Ebn Touhami, *Der Pharm. Chem.*, **2011**, 3, 272.
- [16] A. Zarrouk, B. Hammouti, A. Dafali, H. Zarrok, *Der Pharm. Chem.*, **2011**, 3, 266.
- [17] A. Ghazoui, R. Saddik, N. Benchat, B. Hammouti, M. Guenbour, A. Zarrouk, M. Ramdani, *Der Pharm. Chem.*, **2012**, 4, 352.
- [18] D. Ben Hmamou, R. Salghi, A. Zarrouk, B. Hammouti, S. S. Al-Deyab, Lh. Bazzi, H. Zarrok, A. Chakir, L. Bammou, *Int. J. Electrochem. Sci.*, **2012**, 7, 2361.
- [19] A. Zarrouk, B. Hammouti, H. Zarrok, M. Bouachrine, K. F. Khaled, S. S. Al-Deyab, *Int. J. Electrochem. Sci.*, **2012**, 6, 89.
- [20] A. Zarrouk, B. Hammouti, H. Zarrok, I. Warad, M. Bouachrine, *Der Pharm. Chem.*, **2011**, 3, 263.
- [21] A. H. Al Hamzi, H. Zarrok, A. Zarrouk, R. Salghi, B. Hammouti, S. S. Al-Deyab, M. Bouachrine, A. Amine, F. Guenoun, *Int. J. Electrochem. Sci.*, **2013**, 8, 2586.
- [22] A. Ghazoui, N. Bencat, S. S. Al-Deyab, A. Zarrouk, B. Hammouti, M. Ramdani, M. Guenbour, *Int. J. Electrochem. Sci.*, **2013**, 8, 2272.
- [23] D. Ben Hmamou, R. Salghi, A. Zarrouk, M. Messali, H. Zarrok, M. Errami, B. Hammouti, Lh. Bazzi, A. Chakir, *Der Pharm. Chem.*, **2012**, 4, 1496.
- [24] A. Zarrouk, H. Zarrok, R. Salghi, N. Bouroumane, B. Hammouti, S. S. Al-Deyab, R. Touzani, *Int. J. Electrochem. Sci.*, **2012**, 7, 10215.
- [25] H. Bendaha, A. Zarrouk, A. Aouniti, B. Hammouti, S. El Kadiri, R. Salghi, R. Touzani, *Phys. Chem. News*, **2012**, 64, 95.
- [26] J. Hmimou, A. Rochdi, R. Tourir, M. Ebn Touhami, E. H. Rifi, A. El Hallaoui, A. Anouar, D. Chebab, *J. Mater. Environ. Sci.*, **2012**, 3, 543.
- [27] Y. Aouine, M. Sfaira, M. Ebn Touhami, A. Alami, B. Hammouti, M. Elbakri, A. El Hallaoui, R. Tourir, *Int. J. Electrochem. Sci.*, **2012**, 7, 5400.
- [28] B. Zerga, B. Hammouti, M. Ebn Touhami, R. Tourir, M. Taleb, M. Sfaira, M. Bennajeh, I. Forssal, *Int. J. Electrochem. Sci.*, **2012**, 7, 471.
- [29] M. Cenoui, N. Dkhireche, O. Kassou, M. Ebn Touhami, R. Tourir, A. Dermaj, N. Hajjaji, *J. Mater. Environ. Sci.*, **2010**, 1, 84.
- [30] K. Adardour, O. Kassou, R. Tourir, M. Ebn Touhami, H. ElKafsaoui, H. Benzeid, E. M. Essassi, M. Sfaira, *J. Mater. Environ. Sci.*, **2010**, 1, 129.
- [31] M. Elbakri, R. Tourir, M. Ebn Touhami, A. Srhiri, M. Benmessaoud, *Corros. Sci.*, **2008**, 50, 1538.
- [32] J. Aljourani, K. Raeissi, M. A. Golozar, *Corros. Sci.*, **2009**, 51, 1836.
- [33] M. Lebrini, M. Traisnel, M. Lagrenee, B. Mernari, F. Bentiss, *Corros. Sci.*, **2008**, 50, 473.
- [34] B. B. Damaskin, A. N. Frumkin, N. S. Hush (Ed.) Adsorption of molecules on electrodes, Wiley-Interscience, London, **1971**, p. 1.
- [35] A. D. Becke, *J. Chem. Phys.*, **1992**, 96, 9489.
- [36] A. D. Becke, *J. Chem. Phys.*, **1993**, 98, 1372.

- 
- [37] C. Lee, W. Yang, R.G. Parr, *Phys. Rev. B.*, **1988**, 37, 785.
- [38] Gaussian 03, Revision B.01, M. J. Frisch, et al., Gaussian, Inc., Pittsburgh, PA, **2003**.
- [39] I.N. Putilova, S.A. Balezin, U.P. Baranik, *Metallic Corrosion inhibitor*, Pergamon Press, New York, **1960**, 31
- [40] B. Ateya, B. El-Anadauli, F. El Nizamy, *Corros. Sci.*, **1984**, 24, 509.
- [41] XH .Li, SD. Deng, GN. Mu, H. Fu, FZ .Yang, *Corros. Sci.*, **2008**, 50, 420.
- [42] X. Li, S. Deng, H. Fu, T. Li, *Electrochim. Acta.*, **2009**, 54, 4089.
- [43] E. Cano, JL. Polo, A. La Iglesia, JM. Bastidas, *Adsorption.*, **2004**, 10, 219.
- [44] A. Yurt, A. Balaban, S. Ustün Kandemir, G. Bereket and B. Erk, *Mater. Chem. Phys.*, **2004**, 85, 420.
- [45] M.A. Deyab, S.T. Keera, S.M. El Sabagh, *Corros. Sci.*, **2011**, 53, 2592.
- [46] S. Tamil Selvi, V. Raman and N. Rajendran, *J. Appl. Electrochem.*, **2003**, 33, 1175.
- [47] H. Ju, Z.P. Kai, Y. Li, *Corros. Sci.*, **2008**, 50, 865.
- [48] M. J. S. Dewar, W. Thiel, *J. Am. Chem. Soc.*, **1977**, 99, 4899.
- [49] A.Y. Musa, A. H. Kadhun, A. B. Mohamad, A.b. Rohoma, H. Mesmari, *J. Mol. Struct.*, **2010**, 969, 233.
- [50] M.A. Amin, K.F. Khaled, S.A. Fadl-Allah, *Corros. Sci.*, **2010**, 52, 140.
- [51] E.E. Ebenso, D.A. Isabirye, N.O. Eddy, *Int. J. Mol. Sci.*, **2010**, 11, 2473.
- [52] O. Kikuchi, *Quant. Struct.-Act. Relat.*, **1987**, 6, 179.